



Design and Analysis of Ridge and Sub-Wavelength Grating Waveguide Based Micro Ring-Resonator Sensor

Muhammad Favad Qadir ^{a, *}, Muhammad Mahmood Ali^b

^a Department of Electrical and Computer Engineering, Air University, Islamabad (fawad.qadir@mail.au.edu.pk)

^b Department of Mechatronic Engineering, Atlantic Technological University Sligo Ireland (Muhammad.ali@atu.ie)

Submitted
04-Feb-2024

Revised
06-May-2024

Published
10-Jun-2024

Abstract

The microring resonators assisted with subwavelength grating designs shows great promise in optical sensing and communication. However, its spectrum nature makes it unsuitable for tracking or extracting a single wavelength from a broadband light source. In this paper, we used side-mode suppression, based on microring resonator assisted with subwavelength gratings which offer high flexibility in wavelength design within the silicon-on-insulator (SOI) waveguide. By periodically arranging silicon waveguide pieces in three different widths, we can set the effective index along the inner sidewall of subwavelength microring resonator. Thereby can achieve the precise wavelength selection. We examine the effects of various key parameters on the center wavelength, side-mode suppressed ratio, and coupling gap (CG) of this sensor. The proposed structure is also analysed for coupling strength between the bus and subwavelength grating ring resonator. The wavelength selection, compact size, compatibility with other similar nature waveguide-based devices and design flexibility highlight its significance in integrated optical sensing and optical communication.

Keywords: SOI, Ridge waveguide, Sub-wavelength waveguide, SOI Sensor, Integrated Sensor

* Corresponding Author: Muhammad Favad Qadir (fawad.qadir@mail.au.edu.pk)

1. Introduction

The structures with subwavelengths has garnered significant research work in past few years due to its effective suppression of diffraction effects, achieved through the use of subwavelength based silicon pitches. Its unique characteristics and design flexibility have led to the proposal of various SWG structure-based devices, including optical demultiplexers, polarization beam splitters, mode converters, contra directional couplers, and others.[1, 2] Among these, the subwavelength grating microring resonator (SWGMR)-based filter has demonstrated impressive performance in biosensing and communication applications despite its limitations [3, 4].

For sensors normally based on single-ring resonator, measurements typically dependent on variation of the resonant wavelength, which can be significantly constrained by the FSR, especially under conditions requiring high sensing sensitivity [5]. The larger ring radius provide contact with the external environment but results in a narrower FSR and reduced measurement range. Additionally, for optical sensors using microring resonators, the comb spectrum poses limitations when light source is not consist on single wavelength, such as in broadcast that consists on multicast wavelength division multiplexing [6]. Using additional filters increases system complexity. Furthermore, side-mode suppressed microring resonator (MRR) filters reported to date are based on channel waveguides, requiring suitable couplers to connect the subwavelength waveguides, making them unsuitable for device integration [7-9]. Although techniques such as neural network [10] is being used but it is complex.

To address these issues, we propose enhancing the traditional SWG-MRR to suppress side modes and retain only the target wavelength using Ridge bus waveguide coupling. Notably, there has been prior work on side-mode suppressed SWG-MRRs but coupling strength and sensing analysis with different coupling gaps (CGs) and MMI like coupling section with the help of ridge waveguide is not demonstrated. In this paper, we introduce and analyse the side-mode suppressed sensor based on an angular grating assisted-subwavelength-MRR (AG-SWGMR) for generic sensing and optical communication applications. This sensor allows two flexible wavelength filtering by simply adjusting the widths of three types of silicon waveguide pieces arranged periodically to present the effect of effective index modulation on the inner side of the SWG-MRR.

We employ the 2.5 D finite-difference time domain (FDTD) method with mesh accuracy of 4 to simulate the output transmission response and evaluate the overall structural performance. We examine and discuss the variations in centre-wavelengths and side-mode suppression, sensing analysis in relation to coupling gap and change in refractive index.

2. Structure Design

The schematic of proposed grating assisted subwavelength based micro ring resonator is shown in Figure 1. The thickness of silicon layer is 220 nm ($n = 3.46$) that is built on silica layer ($n = 1.44$). The cladding is air with

$n = 1$. The incoming light ridge waveguide width is 500 nm so that it supports only the fundamental mode which is TE polarized. The ring radius is set as 8.5 μm , and the ring comprises 148 Si pieces. Unlike conventional SWG-MRRs, this design uses three types of silicon pieces to modulate the effective index along the ring waveguide, and act as gratings in the inner wall of the subwavelength ring. The Si pieces have widths denoted as P1, P2, and P3, each with inner and outer widths of 225 nm, optimized to 490 nm, 690 nm, and 890 nm, respectively.

The coupling gap between bus waveguide and the ring waveguide is set to 0 nm with incorporation of 77 nm width of a coupling joint to achieve desired coupling. MODE Solutions software is used for simulation, employing a 2.5D FDTD method suitable for structures that are not changing their dimension in a particular direction, like this angular grating-subwavelength-MRR, providing reliable results with less computational intensity compared to 3D counterparts.

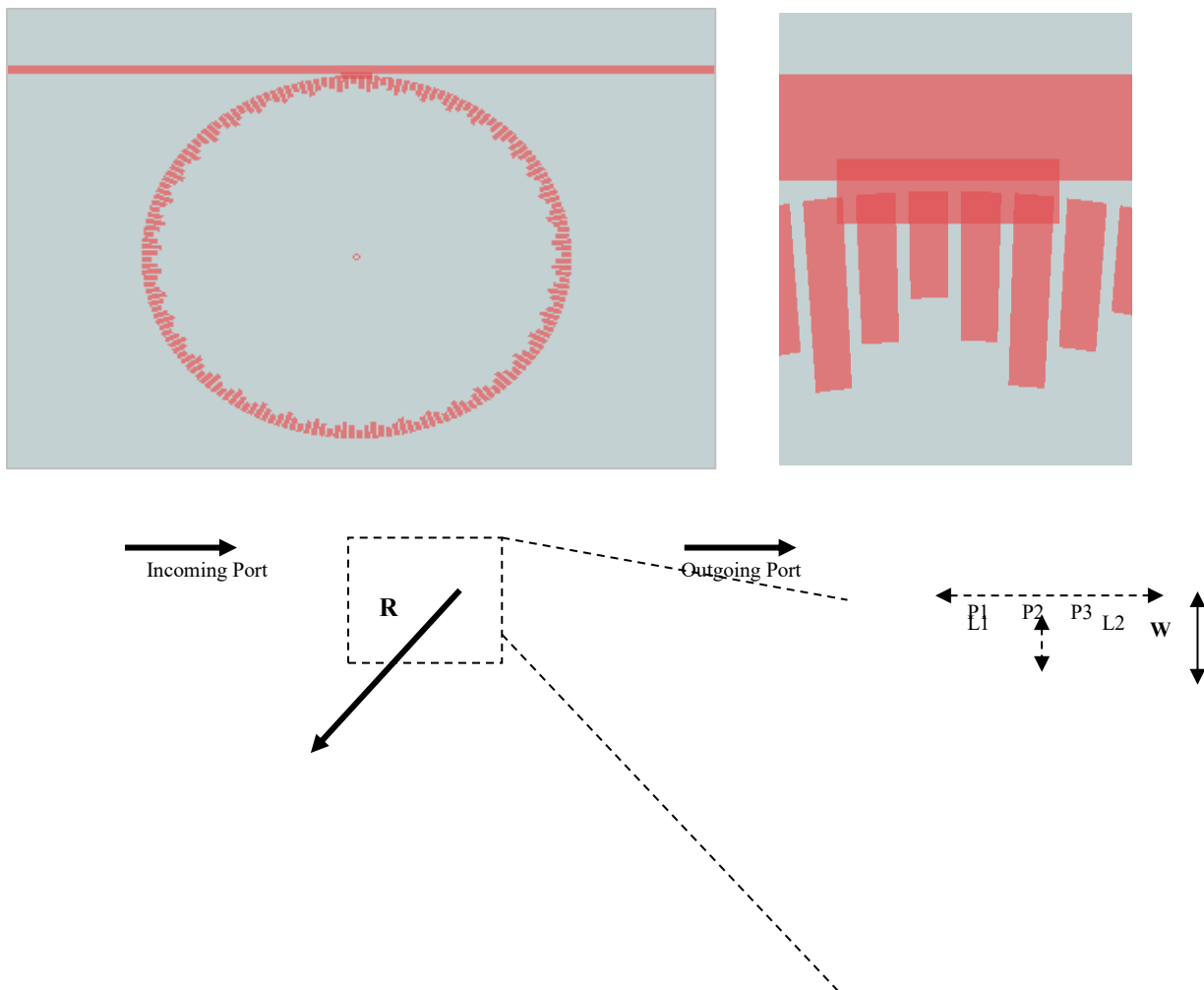


Figure 1: Schematic of proposed Ridge and sub-wavelength grating based micro-ring resonator sensor

The simulation is performed with varFDTD solver with accuracy setting regarding mesh is 4, balancing accuracy, incorporating memory requirements and simulation time. Further for perfectly matched layer (PML)

settings, choosing a stretched coordinate PML type and stabilizing the x-axis direction profile with an increased layer of 68. The simulation time should be set at 4000 ps and a minimum auto shutoff is set at 10^{-7} to ensure sufficient calculation time. A field and power monitor at the outgoing port is connected to collect transmission information. We can find the relationship between the resonant wavelength and effective index from Equation 1, where m represents the order of modes [11, 12].

$$m\lambda_{res} = n_{eff} \cdot L \tag{1}$$

The blue line in Figure. 2 shows the spectrum of conventional micro-ring resonator. By selecting appropriate parameters, we can suppress the side modes as in the ring resonator spectrum by the angular grating incorporated ring waveguide's inner sidewall to achieve the selective wavelength characteristic and side-mode suppression. Similar to conventional MRRs, effective index modulation in a Bragg angular grating can be achieved through the alternative arrangement of silicon pieces having different widths after careful optimization.

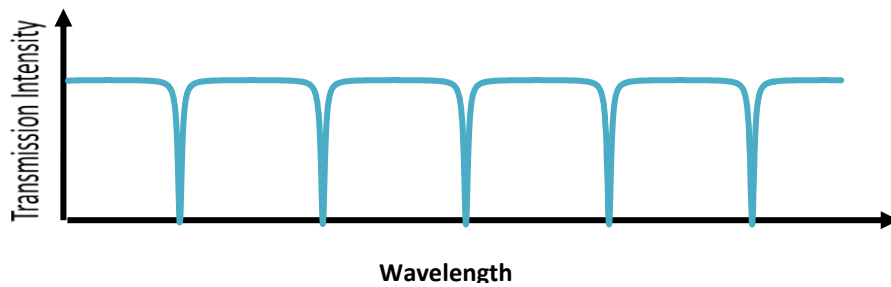


Figure 2: Transmission spectrum of conventional micro-ring resonator

Figure. 3 shows the spectral response of sub-wavelength grating micro-ring resonator, with larger extinction ratio at wavelength 1551 nm and 1564 nm, respectively. The losses occur from coupling loss, losses due to propagation, and bending loss of the subwavelength-ring waveguide.

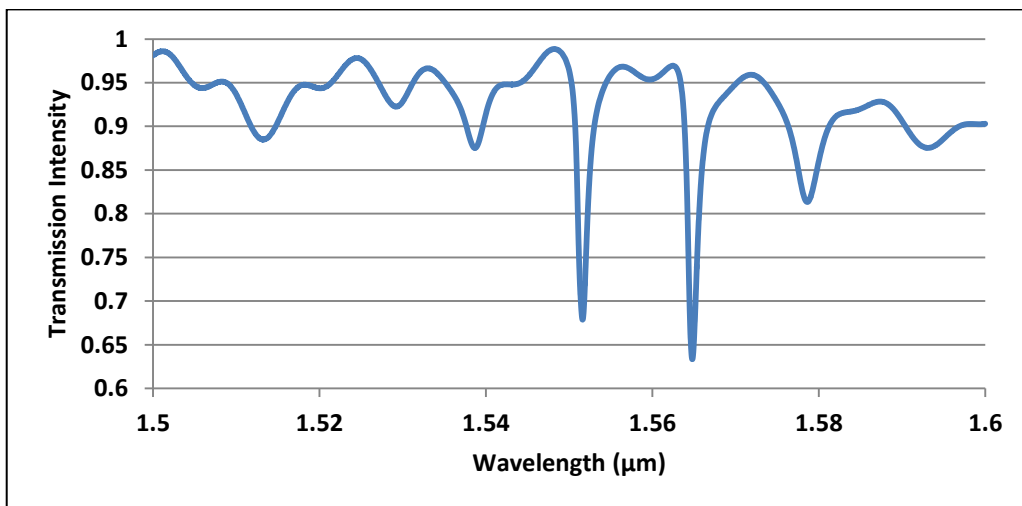


Figure 3: Transmission spectrum of proposed structure at output port

3. Parametric Optimization

As the coupling gap (CG) in a silicon-on-insulator (SOI) ring resonator structure plays a crucial role in determining the device's performance, particularly in terms of coupling efficiency, resonance characteristics, and overall sensitivity. We investigate our design with different values of coupling gaps and take the transmission spectrum accordingly as shown in Figure 4. The results show that a smaller coupling gap results in stronger coupling, which can enhance the transfer of light from the bus waveguide into the ring resonator. This increased coupling can lead to a higher resonance peak and improved sensitivity for applications such as sensing and filtering.

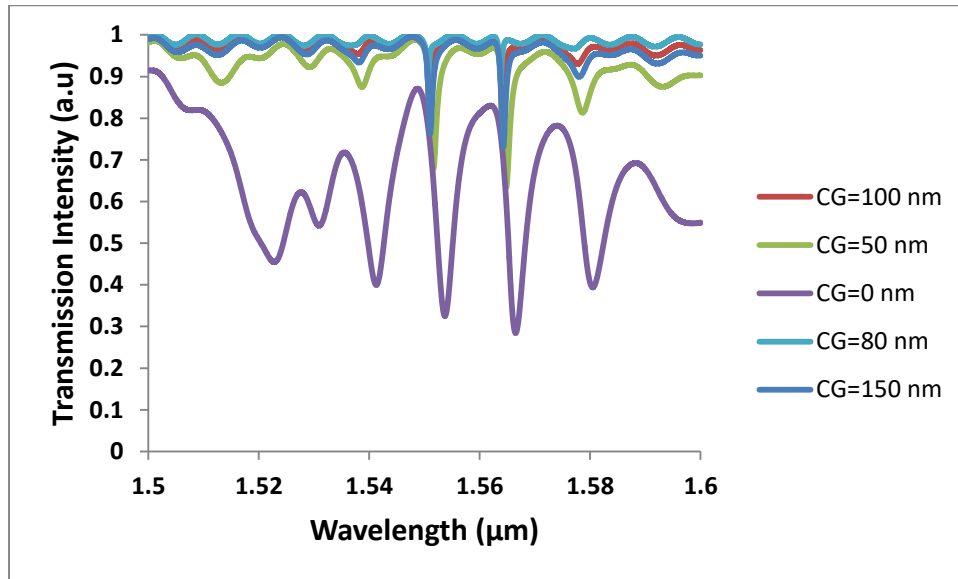


Figure 4: Transmission spectrum for varying Coupling Gaps (CGs)

An excessively small coupling gap can also introduce significant challenges. For instance, it can increase the insertion loss due to higher propagation losses and scattering at the coupling region. This can degrade the overall quality factor (Q-factor) of the resonator, reducing its efficiency and performance in practical applications. As shown in Figure.4 violet color spectrum is transmission spectrum for zero coupling gap. Additionally, fabricating extremely small coupling gaps with high precision is technologically demanding and may lead to fabrication inconsistencies, further impacting device performance. Conversely, a larger coupling gap results in weaker coupling, which might be beneficial for reducing insertion loss and improving the Q-factor. However, it can also reduce the coupling efficiency, making it difficult to achieve the desired resonance conditions. This can limit the effectiveness of the resonator in applications requiring precise wavelength filtering or high sensitivity. Here we have a larger coupling gap of about 150 nm showing in light blue color in Figure 4.

Therefore, optimizing the coupling gap in SOI ring resonator structures is a delicate balance. It requires careful consideration of the trade-offs between coupling efficiency, insertion loss, and fabrication feasibility. Advanced simulation tools and precise fabrication techniques are essential for determining the optimal coupling gap that maximizes performance for specific applications. By carefully controlling the coupling gap, designers can

enhance the functionality of SOI ring resonators in various optical communication and sensing applications, ensuring high performance and reliability.

4. Applications

Our proposed grating assisted subwavelength-ring resonator presents a highly promising solution for silicon-on-insulator (SOI) based sensing applications [13-16]. The unique design of the SWG structure, characterized by its periodic arrangement of silicon pillars, enables precise modulation of the effective index within the ring waveguide. This capability allows for highly selective wavelength filtering, crucial for accurate sensing. The integration of SWG technology in an SOI platform leverages the high refractive index contrast and mature fabrication processes of silicon photonics, ensuring compact device dimensions and compatibility with existing optical components. Furthermore, the subwavelength grating enhances light-matter interaction within the resonator, thereby increasing sensitivity and enabling the detection of minute changes in the refractive index of the surrounding environment [17-19]. This makes the SWG-based ring resonator particularly suitable for biosensing and chemical sensing applications[1] as shown in Figure. 5, where detecting small variations in analyze concentration is critical. In Figure 5, we can see that when refractive index varies from 1 to 1.3 the resonating wavelength also shifts toward the larger values of wavelength. The side-mode suppression achieved with our design further ensure that the resonator can deliver reliable and high-resolution sensing performance. Thus, our SWG-based ring resonator can improves the efficiency and sensitivity of SOI-based sensing systems.

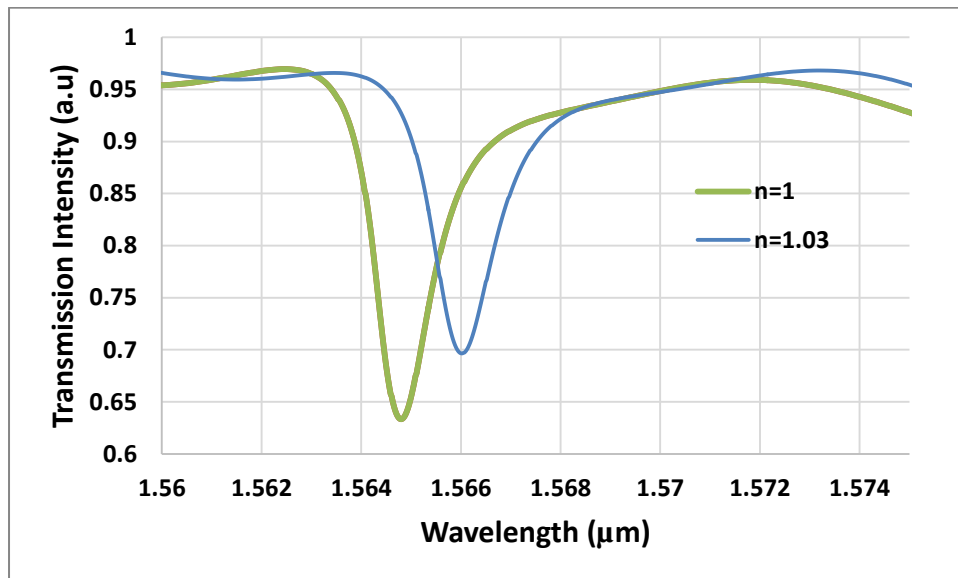


Figure 5: Red shift in wavelength when RI changes from 1 (air) to 1.03 (Chemical gases range)

5. Conclusion

To summarize, we have developed a side mode suppressed sensor based on an angular grating-sub wavelength grating MRR, offering good flexibility in wavelength design. Simulations using the FDTD method show that periodically arranged silicon pillars with three different widths effectively modulate the index along the sub wavelength grating MRR's inner side, enhancing the center wavelength design and SMSR. It also shows great potential for sensing systems. This structure is promising for compact integrated sensing and communication systems.

Acknowledgements

We gratefully thank Dr. Muhammad Awais and Dr. Zohaib for their insightful discussions and mentorship.

References

- [1] C. A. Barrios, "Optical Slot-Waveguide Based Biochemical Sensors," *Sensors*, vol. 9, no. 6, pp. 4751-4765, 2009.
- [2] Y. Chang, and Y. Jiang, "Highly Sensitive Plasmonic Sensor Based on Fano Resonance from Silver Nanoparticle Heterodimer Array on a Thin Silver Film," *Plasmonics*, vol. 9, no. 3, pp. 499-505, 2014/06/01, 2014.
- [3] C.-Y. Chao, and L. Guo, "Biochemical Sensors Based on Polymer Microrings with Sharp Asymmetrical Resonance," *Applied Physics Letters*, vol. 83, 08/25, 2003.
- [4] J. Jung, H. Nam, B. Lee, J. O. Byun, and N. S. Kim, "Fiber Bragg Grating Temperature Sensor with Controllable Sensitivity," *Applied Optics*, vol. 38, no. 13, pp. 2752-2754, 1999.
- [5] M.-S. Kwon, and W. H. Steier, "Microring-resonator-based Sensor Measuring both the Concentration and Temperature of a Solution," *Optics Express*, vol. 16, no. 13, pp. 9372-9377, 2008/06/23, 2008.
- [6] X. Li, L. V. Nguyen, M. Becker, H. Ebendorff-Heidepriem, D. Pham, and S. C. Warren-Smith, "Simultaneous Measurement of Temperature and Refractive Index Using an Exposed Core Microstructured Optical Fiber," *IEEE Journal of Selected Topics in Quantum Electronics*, vol. 26, no. 4, pp. 1-7, 2020.
- [7] P. Liu, and Y. Shi, "Simultaneous Measurement of Refractive Index and Temperature using a Dual Polarization Ring," *Applied Optics*, vol. 55, no. 13, pp. 3537-3541, 2016.
- [8] P. Liu, and Y. Shi, "Simultaneous Measurement of Refractive Index and Temperature using Cascaded Side-coupled Photonic Crystal Nanobeam Cavities," *Optics Express*, vol. 25, no. 23, pp. 28398-28406, 2017/11/13, 2017.
- [9] H. Luo, Q. Sun, Z. Xu, D. Liu, and L. Zhang, "Simultaneous Measurement of Refractive Index and Temperature using Multimode Microfiber-based Dual Mach-Zehnder interferometer," *Optics Letters*, vol. 39, no. 13, pp. 4049-4052, 2014/07/01, 2014.

- [10] Z. Gou, C. Wang, Z. Han, T. Nie, and H. Tian, "Artificial Neural Networks Assisting the Design of a Dual-mode Photonic Crystal Nanobeam Cavity for Simultaneous Sensing of the Refractive Index and Temperature," *Applied Optics*, vol. 61, no. 16, pp. 4802-4808, 2022.
- [11] T. Ma, L. Sun, J. Yuan, X. Sang, B. Yan, K. Wang, and C. Yu, "Integrated label-free Optical Biochemical Sensor with a Large Measurement Range Based on an Angular Grating-microring Resonator," *Applied Optics*, vol. 55, no. 18, pp. 4784-90, Jun 20, 2016.
- [12] L. M. Ping Lu, Kevin Sooley, and Qiying Chen, "Tapered Fiber Mach-Zehnder Interferometer for Simultaneous Measurement of Refractive Index and Temperature," *Applied Physics Letters*, vol. 94, 2009.
- [13] B. Yin, S. Wu, M. Wang, W. Liu, H. Li, B. Wu, and Q. Wang, "High-sensitivity Refractive Index and Temperature Sensor Based on Cascaded Dual-wavelength Fiber Laser and SNHNS Interferometer," *Optics Express*, vol. 27, no. 1, pp. 252-264, 2019.
- [14] F. Yu, P. Xue, X. Zhao, and J. Zheng, "Simultaneous Measurement of Refractive Index and Temperature Based on a Peanut-Shape Structure In-Line Fiber Mach-Zehnder Interferometer," *IEEE Sensors Journal*, vol. 19, no. 3, pp. 950-955, 2019.
- [15] G. Yuan, L. Gao, Y. Chen, J. Wang, P. Ren, and Z. Wang, "Efficient Optical Biochemical Sensor with Slotted Bragg-grating-based Fabry-Perot Resonator Structure in Silicon-on-insulator Platform," *Optical and Quantum Electronics*, vol. 47, no. 2, pp. 247-255, 2015/02/01, 2015.
- [16] J. Zhang, Q. Sun, R. Liang, W. Jia, X. Li, J. Wo, D. Liu, and P. P. Shum, "Microfiber Fabry-Perot Interferometer for Dual-Parameter Sensing," *Journal of Lightwave Technology*, vol. 31, no. 10, pp. 1608-1615, 2013.
- [17] S. Sikarwar, and B. C. Yadav, "Opto-electronic Humidity Sensor: A Review," *Sensors and Actuators A: Physical*, vol. 233, pp. 54-70, 2015.
- [18] F. Sun, J. Wei, B. Dong, Y. Ma, Y. Chang, H. Tian, and C. Lee, "Coexistence of Air and Dielectric Modes in Single Nanocavity," *Optics Express*, vol. 27, no. 10, pp. 14085-14098, 2019.
- [19] X. Wang, J. Flueckiger, S. Schmidt, S. Grist, S. T. Fard, J. Kirk, M. Doerfler, K. C. Cheung, D. M. Ratner, and L. Chrostowski, "A Silicon Photonic Biosensor Using Phase-shifted Bragg Gratings in Slot Waveguide," *J Biophotonics*, vol. 6, no. 10, pp. 821-8, Oct, 2013.